Advanced Performance Materials, 2, 289–298 (1995)

Structure and Coarsening Behavior of the Strengthening Phase in RS Al-Fe-Mo-Si-Zr-Ti Alloys

S.L. DAI, G.F. YU AND M.G. YAN
Institute of Aeronautical Materials, Beijing 100095

Abstract. The structure, space groups, lattice parameters and stoichiometric formula for the strengthening phase in Al-Fe-Mo-Si-Zr-Ti alloys were determined by X- ray diffraction, TEM, CBED and EDX. The coarsening behavior and mechanism of the strengthening phase were studied also using TEM and EDX. Results showed that the strengthening phase was identified to be BCC $Al_{12}(Fe, Mo, Zr, Ti)_3Si$ ($Im3$, $a = 1.263$ nm) and the coarsening rates is the lowest in all the intermetallic phases of Al-Fe system, which is controlled by the diffusion of alloy element Zr in the matrix. Addition of Gd, Y make a volumetric coarsening rate one order of magnitude slower, at 477°C approaching to the coarsening rate LI_2 $Al_3(Zr, V)$ phase.

Keywords: aluminum alloy, coarsening behavior, rapid solidification

Introduction

In the past two decades, significant interest has been directed to advance aluminum alloys produced by the powder metallurgy (P/M)-rapid solidification (RS) route. A specific target of P/M-RS processes was the development of high-temperature range 150 ~ 400°C [1]. Improvements in the processing conditions have made the alloy's properties attractive, for example, tensile strengths of 450 to 600 MPa are achievable at room temperature, with an elongation to fracture and fracture toughness up to 17% and 25 MPa · $m^{3/2}$ respectively, while at 400°C the tensile strength retained may be as high as 250 MPa. Among the most successful development alloy system are Al-Fe-V-Si(8009, 8022) and Al-Fe-X(8019) produced by several different atomization techniques [2, 3]. These alloys could be utilized over a wide range of aircraft and space vehicle.

In order to fulfill the necessity and design requirements of the advanced aerospace vehicle and propulsion systems, in addition to the Al-Fe-V-Si and Al-Fe-Ce alloys, development of new Al alloy systems to be used above a temperature of 427°C(800 F) became an active field of research in the past five years [4]. According to experimental exploration by the present authors it is found that a new Al-Fe-Mo-Si-Zr-Ti alloy system with a new strengthening phase may hold good promise for this kind of application. In this paper, the strengthening phase and its coarsening behavior and mechanism of this alloy system are presented.

Experimental

The composition of the alloy powders produced by USGA technique are shown in Table 1. Powders of 40 μm or less were vacuum-degassed, hot-pressed and extruded at a 16:1 ratio into a 12.5 mm rod.

Foils for transmission electron microscopy (TEM) were prepared by the double-jet method using an electrolyte of 30% HNO_3 in methanol at 40 V and −30°C. The thin

Table 1. Alloy compositions.

	Alloy amount (wt%) of the following elements:							
	Fe	Mo	Si	Zr	Ti	Gd	Y	Al
1	8.0	1.6	1.5	1.0	0.2	—	—	bal
2	8.0	1.6	1.5	1.0	0.2	0.5	—	bal
3	8.0	1.6	1.5	1.0	0.2	—	0.5	bal

foils were examined in Jeol 2000FX scanning TEM(STEM) equipped with a Link systems 860 energy-dispersive X-ray analysis (EDX) spectrometer. Analysis by EDX were quantified using the Link systems RTS-2/FLS computer program.

To aid phase identification, X-ray analysis was conducted using a D/max-rB diffractometer with Cu Kα radiation.

Results and discussion

Identification of the strengthening phases in Alloy 1

The as-solidified microstructure of $5 \sim 74$ μm powders was studied using OP, SEM, TEM and X-ray diffraction in detail [5]. Results shows that powders of 40 μm or less exhibit mixed microcellular and cellular microstructure.

X-ray diffraction studies was performed in as-extruded alloys. A typical X-ray diffraction pattern showing the variation of intensity(cps) as a function of 2θ is presented in Fig. 1 for the Alloy 1. It shows that hot-press and extrustion lead to precipitation of fine precipitate in α-Al matrix. All the precipitate reflections could be consistently indexed on the basis of a BCC lattice ($h + k + l = 2n$) with $a = 1.262$ nm, which closely matches the value of 1.256 nm for the BCC α-AlFeSi compound [6], and that of the precipitates reported in Al-Fe-V-Si alloys [2].

Figure 2a shows typical TEM images of the strengthening phase precipitates in Alloy 1 when aged at 427°C for 2 h. The microstructure consisted of a refined dispersion of pricipitates. The size of the precipitates was about 50 nm. Further aging to 125 h produced no apparent change in the microstructure (Fig. 2b) and showed certain degree of particle coarsening.

Electron diffraction studies were carried out to confirm the X-ray results. Examples of diffraction patterns recorded from individual precipitates are shown in Fig. 3. These and all other patterns could be consistently indexed on the basis of a BCC lattice with a lattice paramerter almost identical to that determined by X-ray diffraction. CBED pattern for the strengthening phase precipitate from [025] zones are shown in Fig. 4a,b. Both whole pattern symmetry and bright field symmetry are m, which gives the possible diffraction group as m, $m1_R$ and $2_R mm_R$. For the BCC lattice and $\langle uv0 \rangle$ zone axes, no m, ml_R diffraction groups existed, therefore the diffraction group of the precipitates should be $2_R mm_R$, and the point group corresponding to the diffraction group is $m3$ [7].

The possible space groups for this point group are $Pm3$, $Pn3$, $Pa3$, $Fd3$, $Im3$, and $Ia3$ [7]. Since the lattice is BCC, the choice of space groups is reduced to the last two, namely, $Im3$ or $Ia3$. For the latter space group, reflections of type $0kl$ for which k and l

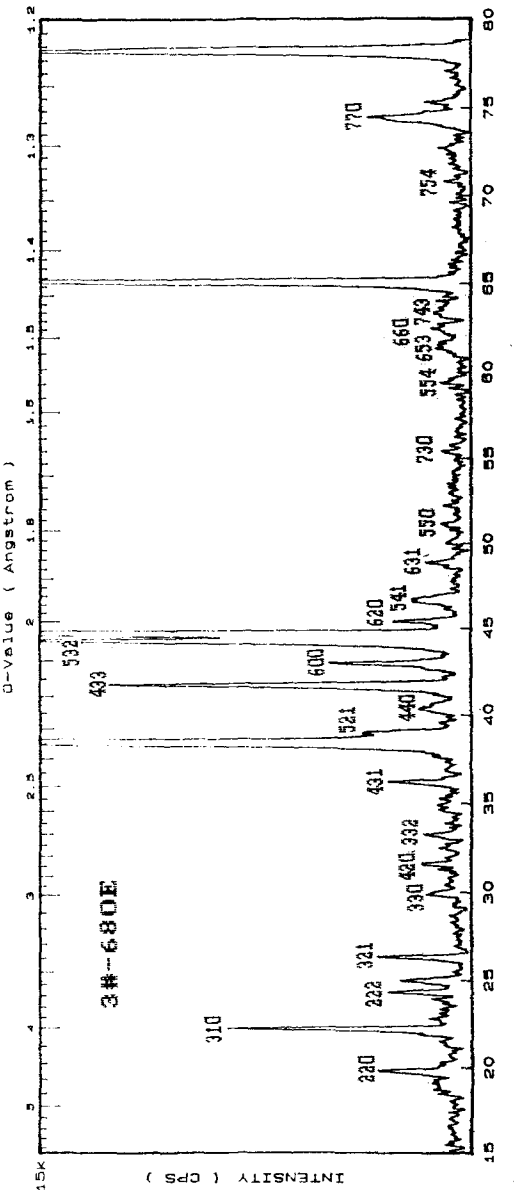

Figure 1. A typical X-ray diffraction pattern for Alloy 1: variation of intensity as a function of 2θ in as-extruded condition.

Table 2. Comparison of composition of the strengthening phase with of the cubic α-AlFeSi compound.

$Al_{12}(Fe, Mo, Zr, Ti)_3Si$						BCCα-AlFeSi		
Al	Fe	Mo	Zr	Ti	Si	Al	Fe	Si
	15.76	1.55	1.19	0.97				
75.07		19.47			5.46	75.0	18.8	6.2

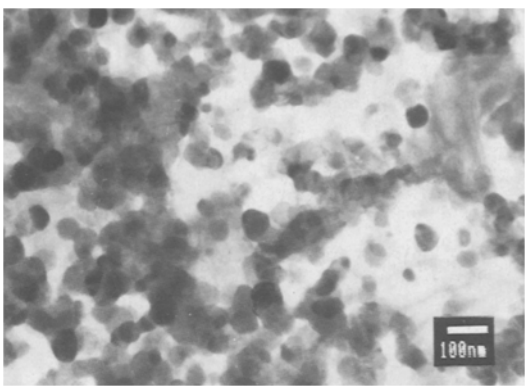

(a)

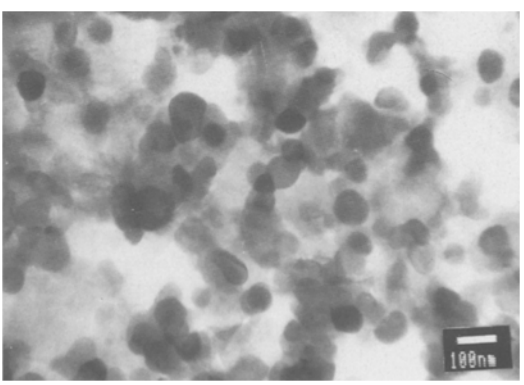

(b)

Figure 2. Typical bright field micrographs of the strengthening phase in Alloy 1: (a) aging at 427°C, (b) aging at 427°C for 125 h.

are not multiples of 2, i.e. the type 011, $0\bar{1}1$, 033, $0\bar{3}3$ ..., are forbidden, which is not the case here. Thus, the space group of the precipitate is unambiguously established as $Im3$, in agreement with that reported for the cubic α-AlFeSi compound [6].

EDX microanalysis of the strengthening phase was carried out, which reveals that the phase contains Al, Fe, Mo, Si, Zr and Ti. The average composition of the precipitates based on analysis of thirty particles, is given in Table 2, together with that reported [6] for the

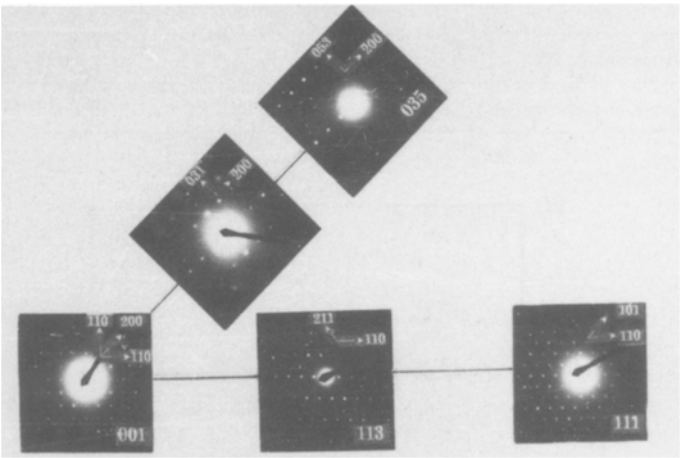

Figure 3. Examples of electron diffraction patterns recorded from individul precipitates.

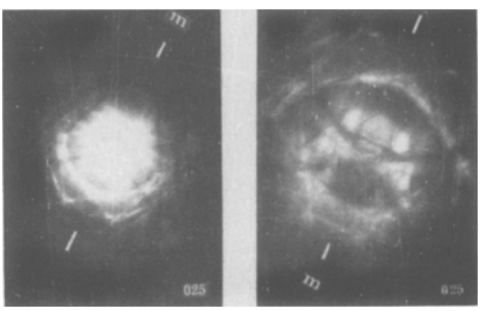

(a) (b)

Figure 4. CBED patterns taken from [025] the strengthening phase: (a) whole pattern symmetry, (b) bright field symmetry.

cubic α-AlFeSi compound. It is evident that the compositions determined in this study are in excellent agreement.

The cubic α-AlFeSi($Al_{12}Fe_3Si$) compound is complex with 138 atoms per unit cell [6]. The equilibrium α-AlFeSi compound has an HCP structure with $c = 2.62$ nm and $a = 1.23$ nm, but is modified to be the cubic form with a in the range of 1.25 to 1.27 nm by the presence of minor amounts of transition elements, notably Mn, V, Cr, W, and Mo substituting for the Fe. Thus, on the assumption that the Mo, Zr, Ti atoms partially substitute for the Fe, the stoichiometry formula for the strengthening phase is obtained as $Al_{12}(Fe, Mo, Zr, Ti)_3Si$.

Coarsening kinetics of the strengthening phase in Alloy 1

The coarsening kinetics of the strengthening phase in Alloy 1 were determined at 427°C, 477°C, and 527°C by TEM and EDX. Figure 5 shows the results at 427°C, 477°C, and

Table 3. Measured volumetric coarsening rate constants K for the strengthening phase in Alloy 1 aged at 427, 477 and 527°C.

Temperature (°C)	427	477	527
Coarsening rate (m^3/h)	2.35×10^{-26}	2.04×10^{-26}	5.76×10^{-26}

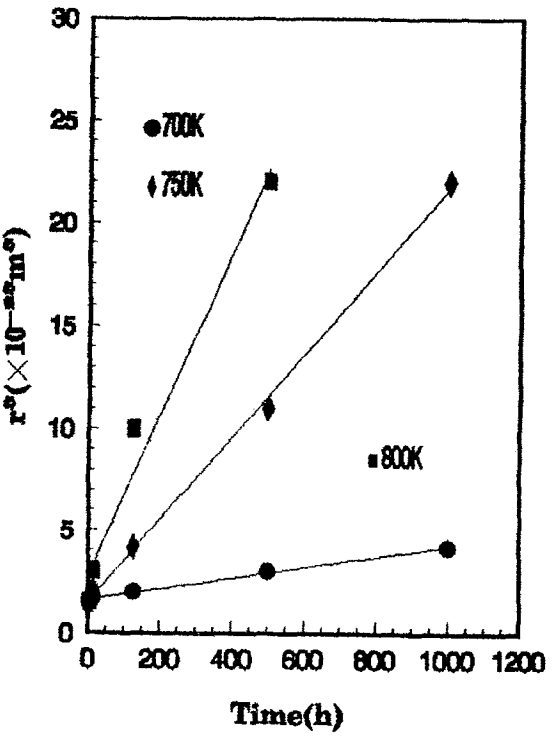

Figure 5. Coarsening kinetic of the strengthening phase at various temperature in Alloy 1.

527°C, where the cube of the average particle radius, based on analysis of 400 particles, is plotted against aging time, in which the linear correlation coefficient is greater than 0.997.

The coarsening behavior of the strenghening phase at 427°C, 477°C, and 527°C shows good agreement with r_3 vs t relationship, $r_3 - r_0^3 = Kt$, which suggests that an LSW-type volume diffusion controlling process [8] is the coarsening mechanism. Here r is the average particle radius after aging for time t and r_0 is an integration constant. K is the coarsening rate, for the stengthening phase at 427°C, 477°C and 527°C are shown in Table 3. If the effect of the precipitate volume fraction on Ostwald ripening is taken into account, the coarsening rate constant K for an alloy containing ϕ of precipitates is given by [8]

$$K = \frac{6\gamma C \cdot DV_m^2}{RT} \cdot f(\phi) \tag{1}$$

Where γ is the interfacial energy, V_m is the molar volume of the precipitate, R is the gas constant and D is the lattice diffusion coefficient. This equation has been used by others to

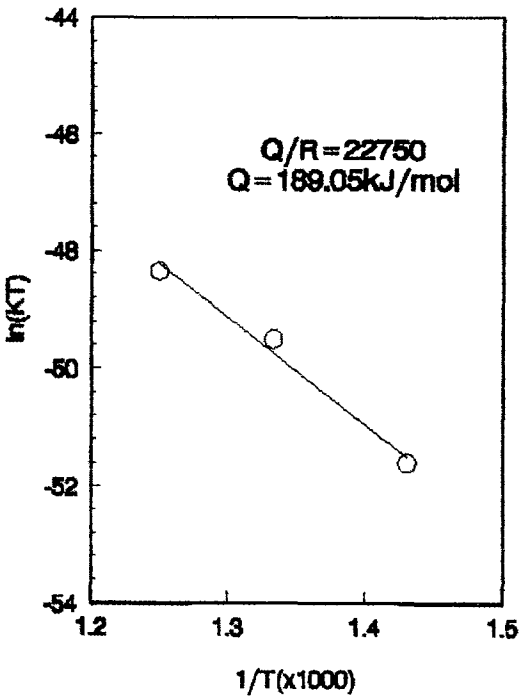

Figure 6. Plat of $\ln(KT)$ vs $1/T$ for the coarsening of the strengthening phase in Alloy 1.

determine the activation energy of diffusivity of solute in the matrix from the experimental coarsening results [9]. After rearrangement, Eq. (1) becomes

$$\ln(KT/C) = \ln A - Q/RT \tag{2}$$

where A is given by

$$A = \frac{6rD_0V_m^2 f(\phi)}{R} \tag{3}$$

and Q is the activation energy of diffusivity for the rate-controlling element in the matrix. The value of A is a slowly varying function of temperature and usually may be regarded as constant over a small temperature range. Therefore, the value of Q can be experimentally determined from a plot of $\ln(KT/C)$ vs the reciprocal of temperature.

In the present alloy, for the strengthening phase Al_{12}(Fe, Mo, Zr, Ti)$_3$Si. Fe, Mo or Zr may be the rate-controlling element, in which Zr is the most possible one because of its slow solid state diffusivity. The concentration C of Zr or of Mo or of Fe in the solid solution Al matrix in equilibrium is very small and has little change against temperature from 400°C to 600°C. For a first order approximation, C is assumed to be constant in the temperature range from 427°C to 527°C. From the plot of $\ln(KT)$vs $1/T$ shown in Fig. 6, Q is calculated to be 189.05 kJ/mol. The value is closer to the activation energy for diffusion of Zr in Al-Fe-Zr-Si alloy, 218 kJ/mol [6], than to the value for Fe, 127.0 kJ/mol and Mo, 55 kJ/mol in Al. Consequently, the volume diffusion of Zr is likely the rate controlling process for the Ostwald ripening of Al_{12}(Fe, Mo, Zr, Ti)$_3$Si, as expected originally.

There is a great mismatch (5%) between the strengthening phase $Al_{12}(Fe, Mo, Zr, Ti)_3Si$ and Al matrix, therefore, the interfacial energy between them can be estimated, i.e. $\lambda = 1\ J/m^2$ [8].

According to the Broilsford and Wynablatt's theory [10], in Eq. 1 when $\phi = 25\%$, $f(\phi) = 2.37$. With $Vm = 1.45 \times 10^6\ m^3/mol$ and approximation of $C \times D$ in Al-Zr alloy, the coarsening rate is calculated to be $1.749 \times 10^{-26}\ m^3/h$. The value is very closer to the experimental coarsening rate, which confirms that Zr is the coarsening rate-controlling element.

Effect of Gd, Y on the coarsening behavior of the strengthening phase

The coarsening kinetics of the strengthening phase in Alloy 2 and Alloy 3 were also determined by TEM and EDX at 427°C, 477°C, and 527°C. Typical microstructures of Alloy 2 and Alloy 3 after 2 h, 12 h, 125 h, 500 h, and 1000 h of aging at 477°C are shown in Fig. 7. There were little changes in the size of the strengthening phase particles. The coarsening behavior of the strengthening phase both in Alloy 2 and Alloy 3 at 477°C and 527°C and

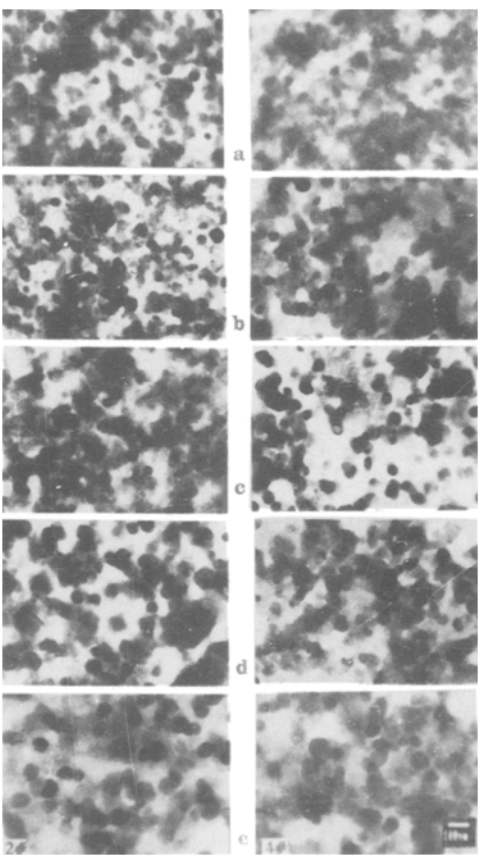

Figure 7. Typical TEM micrographs showing the strengthening phase of Alloys 2 and 3 after aging for (a) 2 h, (b) 12 h, (c) 125 h, (d) 500 h, (e) 1000 h.

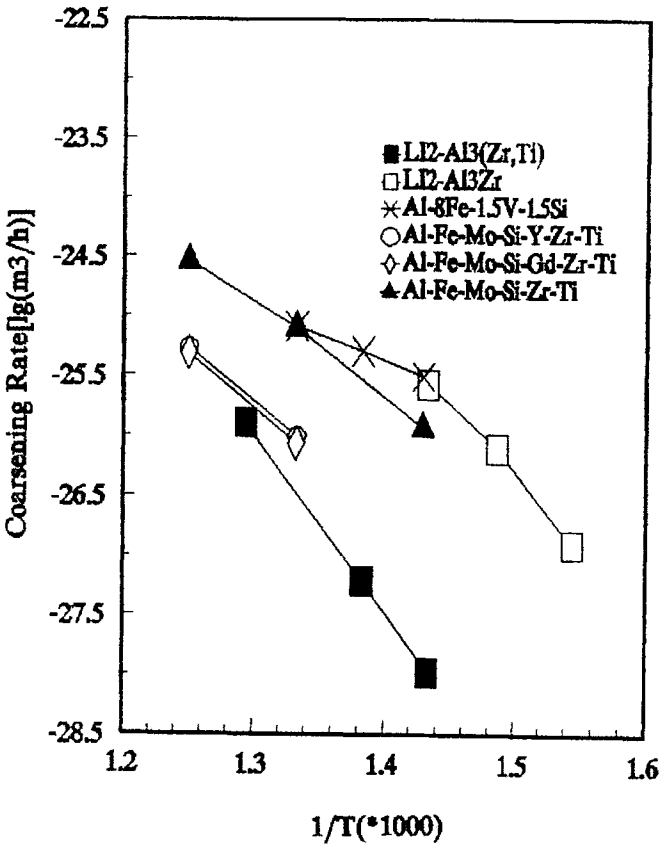

Figure 8. Comparison of volumetric coarsening rate of the stengthening phases in Alloys 1, 2 and 3 with that of $Al_{12}(Fe, V)_3Si$, Al_3Zr and $Al_3(Zr, V)$ phase.

also shows good agreement with r_3 vs t relationship. Figure 8 compares the variation of coarsening rate of the stengthening phase as a function of temperature in the present alloy with that in Al-Fe-V-Si, Al-Zr, and Al-Zr-V alloys after correcting the volume fraction of strengthening phase.

Results show that the coarsening rate of the strengthening phase in Alloy 1 is half order of magnitude slower than that of $Al_{12}(Fe, V)_3Si$ at 427°C and of the strengthening phase in Alloy 2 and Alloy 4 is an order of magnitude slower than that in Alloy 1 and very closer to that of $Al_3(Zr, V)$ in Al-Zr-V alloys. The $Al_3(Zr, V)$ phase is regarded as a promising strengthening phase to realize application of elevated temperature aluminum alloy above 427°C, but only limited by the volume fraction of the phase. Thus, it is expected that the aim of using above 427°C may be realized in Al-Fe-Mo-Si-Zr-Ti-Gd(Y) alloy.

Conclusions

1. The microstructure of rapidly solidified Al-Fe-Mo-Si-Zr-Ti alloy consists of a refined dispersion of spherical strengthening phase precipitates in a Al matrix. It was established

that the strengthening phase Al_{12}(Fe, Mo, Zr, Ti) has a BCC structure with $a = 1.263$ nm and space group $Im3$.

2. Coarsening rate of the strengthening phase is half order of magnitude slower than $Al_{12}(Fe,V)_3Si$ in Al-Fe-V-Si(8009) alloy. The activation energy calculated from the strengthening phase coarsening kinetics is close to that for diffusivity of Zr in the Al matrix, suggesting that volume diffusion of Zr is the rate controlling mechanism for the Ostwald ripening of the strengthening phase.
3. Additions of Gd, Y make a volumetric coarsening rate and order of magnitude slower for the strengthening phase, at 477°C approaching to the coarsening rate of Al_3(Zr, V) phase.

References

1. Das, S.K., Gilman P.G., and Raybould D: Key Eng. Met., 29–31:367, 1989.
2. Skinner, D.J. and Bye, R.L.: Scr. Metall., 20:867, 1986.
3. Lee, D.Y. and Zupon D.E.: Dispersion Strengthened Aluminum Alloy, (Y.W. Kim and W.M. Griffith (eds.)), Metallurgical Society, Warrendale, Pennsylvania; p. 256, 1988.
4. Fine, M.E.: Dispersion Strengthened Aluminum Alloy, (Y.W. Kim and W.M. Griffith (eds.)), Metallurgical Society, Warrendale, Pennsylvania, p. 103, 1988.
5. Dai, S.-L., Yu, G.-F, and Yan, M.-G.: Rare-earth in Aerospace, 4:6, 1993.
6. Mondolfo L.F.: Aluminum Alloys, Butterworths, London, 1976.
7. Steeds, S.W.: Introduction to Analytical Electron Microscopy, (J.J. Goldstein and D.C. Joy (eds.)), Plenum Press, New York, 1979.
8. Vasuderan V.K. and Fraser H.L.: Mater. Sci. Eng., 98:131, 1988.
9. Chen, Y.-C. and Fine, M.E.: Acta Metall., 38(5):771, 1990.
10. Broilsford A.D. and Wynblatt P.: Acta Metall., 27:489, 1979.